



HAL
open science

Thermodynamic Effects on Grade Transition of Polyethylene Polymerization in Fluidized Bed Reactors

Sabrine Kardous, Timothy Mckenna, Nida Sheibat-Othman

► **To cite this version:**

Sabrine Kardous, Timothy Mckenna, Nida Sheibat-Othman. Thermodynamic Effects on Grade Transition of Polyethylene Polymerization in Fluidized Bed Reactors. *Macromolecular Reaction Engineering*, 2020, pp.2000013. 10.1002/mren.202000013 . hal-02749293v1

HAL Id: hal-02749293

<https://hal.science/hal-02749293v1>

Submitted on 12 Nov 2020 (v1), last revised 15 Apr 2021 (v3)

HAL is a multi-disciplinary open access archive for the deposit and dissemination of scientific research documents, whether they are published or not. The documents may come from teaching and research institutions in France or abroad, or from public or private research centers.

L'archive ouverte pluridisciplinaire **HAL**, est destinée au dépôt et à la diffusion de documents scientifiques de niveau recherche, publiés ou non, émanant des établissements d'enseignement et de recherche français ou étrangers, des laboratoires publics ou privés.



Postfach 10 11 61
69451 Weinheim
Germany

Courier services:
Boschstraße 12
69469 Weinheim
Germany

Tel.: (+49) 6201 606 581

Fax: (+49) 6201 606 510

E-mail: macromol@wiley-vch.de

WILEY-VCH

Dear Author,

Please correct your galley proofs carefully and return them no more than four days after the page proofs have been received.

The editors reserve the right to publish your article without your corrections if the proofs do not arrive in time.

Note that the author is liable for damages arising from incorrect statements, including misprints.

Please note any queries that require your attention. These are indicated with a Q in the PDF and a question at the end of the document.

Please limit corrections to errors already in the text; cost incurred for any further changes or additions will be charged to the author, unless such changes have been agreed upon by the editor.

Reprints may be ordered by filling out the accompanying form.

Return the reprint order form by fax or by e-mail with the corrected proofs, to Wiley-VCH : macromol@wiley-vch.de

To avoid commonly occurring errors, please ensure that the following important items are correct in your proofs (please note that once your article is published online, no further corrections can be made):

- **Names** of all authors present and spelled correctly
- **Titles** of authors correct (Prof. or Dr. only: please note, Prof. Dr. is not used in the journals)
- **Addresses** and **postcodes** correct
- **E-mail address** of corresponding author correct (current email address)
- **Funding bodies** included and grant numbers accurate
- **Title** of article OK
- All **figures** included
- **Equations** correct (symbols and sub/superscripts)

Corrections should be made directly in the PDF file using the PDF annotation tools. If you have questions about this, please contact the editorial office. The corrected PDF and any accompanying files should be uploaded to the journal's Editorial Manager site.

Author Query Form

WILEY

Journal MREN
Article mren202000013

Dear Author,

During the copyediting of your manuscript the following queries arose.

Please refer to the query reference callout numbers in the page proofs and respond to each by marking the necessary comments using the PDF annotation tools.

Please remember illegible or unclear comments and corrections may delay publication.

Many thanks for your assistance.

Query No.	Description	Remarks
Q-OO	<p>Open access publication of this work is possible via Wiley OnlineOpen. Information about this is available at: https://authorservices.wiley.com/author-resources/Journal-Authors/licensing-open-access/open-access/onlineopen.html.</p> <p>The cost of publishing your manuscript OnlineOpen may be covered by one of Wiley's national agreements. To find out more, visit https://authorservices.wiley.com/author-resources/Journal-Authors/open-access/affiliation-policies-payments/index.html.</p> <p>Note that eligibility for fee coverage is determined by the affiliation of the primary corresponding author designated at submission. Please log in to your Wiley Author Services account at https://authorservices.wiley.com/ and confirm your affiliation to see if you are eligible.</p> <p>Instructions for placing an OnlineOpen order can be found at: https://authorservices.wiley.com/author-resources/Journal-Authors/open-access/how-to-order-onlineopen.html.</p> <p>To publish your article open access, please complete the order process before completing your proof corrections.</p>	
Q1	Please confirm that forenames/given names (blue) and surnames/family names (vermilion) have been identified correctly.	
Q2	Please provide the highest academic title (either Dr. or Prof.) for all authors, where applicable.	
Q3	Please provide postal code in affiliation 2.	
Q4	Please check all equations have been correctly typeset.	

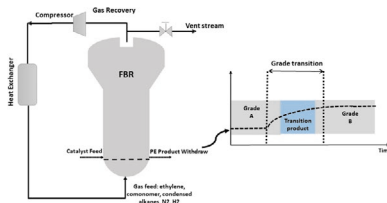
Please confirm that Funding Information has been identified correctly.

Please confirm that the funding sponsor list below was correctly extracted from your article: that it includes all funders and that the text has been matched to the correct FundRef Registry organization names. If a name was not found in the FundRef registry, it may not be the canonical name form, it may be a program name rather than an organization name, or it may be an organization not yet included in FundRef Registry. If you know of another name form or a parent organization name for a "not found" item on this list below, please share that information.

FundRef Name	FundRef Organization Name
Agence Nationale de la Recherche	Agence Nationale de la Recherche

S. Kardous, T. F. L. McKenna,
 N. Sheibat-Othman*2000013

**Thermodynamic Effects on
 Grade Transition of Polyethylene
 Polymerization in Fluidized Bed
 Reactors**



Grade transition is frequent in fluidized bed reactor of polyolefines. The use of model-based optimization tools is essential to decrease the transition product and ensure the required properties. In condensed mode operation, it is important to use a precise thermodynamic model that accounts for the cosolubility effect caused by the induced condensing agent.

UNCORRECTED PROOF

1
2
3
4
5
6
7
8
9
10
11
12
13
14
15
16
17
18
19
20
21
22
23
24
25
26
27
28
29
30
31
32
33
34
35
36
37
38
39
40
41
42
43
44
45
46
47
48
49
50
51
52
53
54
55
56
57
58
59

1
2
3
4
5
6
7
8
9
10
11
12
13
14
15
16
17
18
19
20
21
22
23
24
25
26
27
28
29
30
31
32
33
34
35
36
37
38
39
40
41
42
43
44
45
46
47
48
49
50
51
52
53
54
55
56
57
58
59



Thermodynamic Effects on Grade Transition of Polyethylene Polymerization in Fluidized Bed Reactors

Sabrine Kardous, Timothy F. L. McKenna, and Nida Sheibat-Othman*

An off-line dynamic optimization procedure is employed to optimize the transition between different grades of linear low density polyethylene in a fluidized bed reactor. This type of reactor is frequently operated under condensed mode, which consists of injecting induced condensing agents (ICA) to absorb part of the reaction heat. However, the presence of ICA affects the solubility of monomers in the polymer, so it is important to account for this effect in a grade transition optimization strategy. A kinetic model is combined with a thermodynamic model based on the Sanchez–Lacombe equation of state to describe the grade transitions. Simplified correlations are then suggested to predict the impact of ICA on ethylene and comonomer solubility in a quaternary system. The results highlight the importance of the thermodynamic model during grade transition.

1. Introduction

Polyethylene (PE) is the most widely produced polymer in the world. Among the different types of PE, linear low density polyethylene (LLDPE) occupies an important position with around 30% of the global PE production in 2018.^[1] Most processes used to make LLDPE are gas-phase processes which provide several advantages over slurry processes. Indeed, difficulties related to mass transfer limitations and the dissolution of the amorphous polymer in a diluent, as well as fouling in slurry processes are avoided in gas-phase processes. Gas-phase processes are adequate for multipurpose production and permit the production of a wide range of PE grades. Among gas-phase processes, fluidized bed reactors (FBRs) are far and away the most widely used reactors for the production of LLDPE because they are the only reactors that can remove enough heat in the gas phase and thus allow the production of large amounts of polymer.^[2] In order to further enhance heat transfer and increase productivity, condensed mode cooling is frequently employed, where

induced condensed agents (ICAs), which are typically alkanes such propane or isomers of butane, pentane, or hexane, are injected in either liquid or vapor form.^[3,4] The heat of vaporization and/or increase in the heat capacity of the vapor phase in the reactor absorb a significant amount of the reaction heat and improve the control of the reactor temperature. However, it has also been observed that when the polymer particles are swollen by an alkane or an alkene, the reaction rate can change significantly due to the so-called cosolubility effect. Indeed, the presence of a hydrocarbon heavier than ethylene enhances the solubility of the latter in the amorphous phase of the polymer, thereby contributing to a higher rate of polymeri-

zation, while the lighter hydrocarbons play the role of antisolvent for the heavier ones.^[5,6] Therefore, the presence of ICA increases the ethylene concentration in the particles, leading to a higher reaction rate, while ethylene is expected to act as an antisolvent for the ICAs (and eventually for comonomers like 1-butene or 1-hexene). This is expected to impact the properties of the final product such as its molecular weight and density. Therefore, it is important to account for these effects in the process model, especially in model-based optimization or control strategies.

It is quite common to produce several grades in the same polymerization plant in order to obtain a PE with different density, molecular weight, and polydispersity index required in the various applications of PE.^[7] Frequent transitions between these grades are usually needed to suit the market demand and reduce the storage cost. Due to the long residence time in FBRs, compared to tubular or loop reactors, for instance, the flow rates should be optimized wisely to ensure attaining the new set-point (SP) in a short time, thus reducing the amount of transition product. When condensed mode is employed, the transitions might be more complex since the sorption/desorption dynamics of the different species can change the behavior of the system. The employment of an adapted control of the transition is thus essential in order to optimize the economic yield while ensuring the security of the operations.

Debling et al.^[7] studied the effect of different parameters on grade transition of solution, slurry, bulk, and gas-phase polyolefin reactions in commonly used reactors, including horizontal or vertical stirred beds, loop, and FBRs. They indicated the residence time distribution of the different components to be a determining factor in the speed of grade transition

S. Kardous, N. Sheibat-Othman
Université of Lyon
Université Claude Bernard Lyon 1
CNRS, UMR 5007, LAGEPP, Villeurbanne F-69100, France
E-mail: nida.othman@univ-lyon1.fr

T. F. L. McKenna
Université of Lyon
Université Claude Bernard Lyon 1
CPE Lyon, CNRS, UMR 5265, C2P2 – LCPP group, Villeurbanne, France

The ORCID identification number(s) for the author(s) of this article can be found under <https://doi.org/10.1002/mren.202000013>.

DOI: 10.1002/mren.202000013

1 and summarized the procedures employed to speed the transition in FBRs, such as de-inventorying the reactor content or
2 venting/overshooting the gases at the beginning of the transition. However, they did not investigate the effect of ICA on the
3 residence time of the reactor. Rahimpour et al.^[8] also indicated that partial venting of the reactor, composing a new gas phase
4 and reducing the bed level reduce the quantity of transition product in PE FBRs. They highlighted that such so-called *semi-*
5 *continuous* strategy was necessary in some situations in order to keep the reactor temperature between the gas dew point and
6 the polymer melting point (to avoid agglomeration of the particles), which could not be achieved with the continuous strategy
7 (i.e., by controlling only the flow rates). Note that the flow rates employed during the transition were those used for the
8 final grade, which were calculated by solving the model equations under steady-state (SS) conditions, and identifying the
9 boundary conditions to be implemented for each new grade. However, numerous works indicated that the flow rates of the
10 final grade do not necessarily ensure the best transition, and suggested the employment of dynamic optimization or control
11 algorithms to ensure better transitions.^[9,10]

12 For the particular problem of grade transition in FBRs, most works are based on offline optimization due to the long calculation time and the complexity of problem formulation. McAuley
13 et al.^[11,12] were the first to investigate dynamic optimization of grade transition of PE in gas-phase FBR. They provided a
14 kinetic model for copolymerization, correlations for the final properties based on patent data (i.e., melt index and polymer
15 density), and modeled the FBR as a continuous stirred tank reactor (CSTR) due to its high recycle ratio and low single pass
16 conversion. The suggested control variables were the flow rates of hydrogen and comonomer (1-butene or 1-hexene), as they
17 directly affect the polymer molecular weight and density. Afterward, optimization strategies were proposed for different types
18 of processes, for instance, for slurry high density polyethylene (HDPE) processes composed of two loop reactors^[13] or two
19 CSTRs.^[14]

20 Furthermore, different improvements in the optimization approaches were suggested. For instance, Chatzidoukas et al.^[15]
21 proposed a mixed integer dynamic optimization approach to realize a closed-loop control in a fluidized bed reactor. Nystrom
22 et al.^[16] employed a comparable approach based on dynamic optimization combined to a mixed-integer linear problem related to
23 the sequencing, and solved these decoupled problems by iteration. Bonvin et al.^[17] proposed to employ a measurement-based
24 approach by tracking the necessary conditions of optimality, for instance, based on run-to-run basis, in order to correct for modeling
25 mismatch in a homopolymerization process.

26 Regarding closed-loop control, it was usually considered using algorithms based on an optimization criterion, such as
27 model predictive control (MPC). The closed-loop character of MPC makes it more robust to modeling errors than open-loop
28 dynamic optimization. But, in order to allow its online implementation in FBRs, part of the optimization is usually solved
29 offline. For instance, Wang et al.^[18] combined an offline optimizer and a nonlinear MPC, where the optimal feed rates were
30 calculated offline and the MPC allowed minimizing the modeling error and updating the feed rates. A shrinking horizon
31 nonlinear model predictive control with expanding horizon

least-squares estimation was also implemented to control the grade transition in FBRs.^[19]

2 Among all the cited works, in terms of methodology, dynamic optimization-based policies were the most widely used
3 for gas-phase processes, and they will therefore be employed in this work. Indeed, the optimization criterion is more flexible
4 and can be tuned to optimize instantaneous or cumulative properties during transition, or the transition time. In addition,
5 the previous literature analysis highlights that the parameters that most affect the grade transition are the residence time (distribution)
6 and the hydrogen and comonomer flow rates. However, the thermodynamic interactions that are due to the use of
7 a condensing agent and/or comonomer were not considered. This work is focused particularly on condensed mode, and will
8 explore the implications of using a more representative thermodynamic model than most works that takes into account the
9 interactions between the different species. It is clear that simply using additive solubilities will lead to erroneous conclusions
10 about reaction rates and product properties. It is thus important to understand whether or not this is an important part in
11 optimizing grade transitions.

12 In this work, the grade transition of PE copolymers in a gas-phase FBR operating under condensed mode is considered.
13 First, the effect of ICA (*n*-hexane or iso-butane) on the absorption of monomer (ethylene) and comonomer (1-butene or
14 1-hexene) is investigated using a model based on the Sanchez-Lacombe equation of state (SL EoS) and experimental data
15 from literature.^[20,21] Since no sufficient experimental data are available in the open literature for quaternary systems (i.e., a
16 copolymerization in presence of an ICA), simplifying correlations are proposed in order to allow for fast prediction of the
17 cosolubility effects in a quaternary system.^[21] The thermodynamic correlations are then used to calculate equilibrium
18 solubilities for two copolymerization systems of ethylene with α -olefins. The thermodynamic predictions are combined
19 with kinetic copolymerization models to model the dynamic behavior of the FBR, which is assumed to behave like a single-
20 phase CSTR. The model is valid in the super-dry upper compartment of the FBR, containing only gas and polymer. This
21 dynamic model is finally used within a dynamic optimization strategy to optimize the transitions between different grades
22 of LLDPE.

2. Gas-Phase Catalytic Ethylene Copolymerization Model

2.1. Thermodynamic Model

23 The SL EoS has been used frequently to predict the thermodynamic behavior in binary and ternary systems (polymer plus
24 one or two penetrants, respectively).^[22,23] However, as discussed by McKenna,^[3] solubility data for systems of two penetrants are
25 very scarce, and realistic data for multiple penetrants are totally absent from the open literature. Therefore, in the absence of
26 a reliable data set, we will propose a simplified model accounting for three penetrants (i.e., quaternary system) in an LLDPE
27 plant. Two systems are considered, at 90 °C, which are frequently employed in industry:

- 1 1. Copolymerization of ethylene and 1-hexene in presence of
- 2 *n*-hexane as ICA
- 3 2. Copolymerization of ethylene and 1-butene in presence of
- 4 iso-butane as ICA

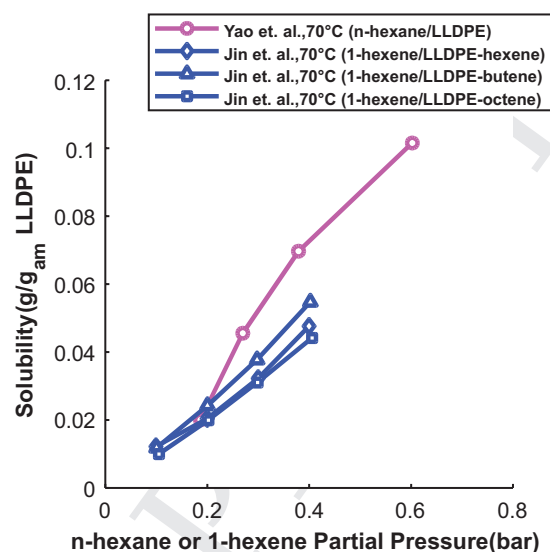
5
6 In the Sanchez-Lacombe EoS, the concentration of the dif-
7 ferent components in the polymer is predicted based on the
8 binary interaction parameters (k_{ij}) between each pair of compo-
9 nents (the penetrating species and the polymer). The thermo-
10 dynamic model is based on the following assumptions: i) The
11 gases dissolve only in the amorphous phase;^[24] ii) There exists
12 no interaction between molecules of olefins and/or ICA.^[25]
13 Thus, in a quaternary system of three penetrating gaseous spe-
14 cies, ethylene (1), ICA (2), and comonomer (3), in the polymer
15 (4), k_{12} , k_{13} , and k_{23} are equal to zero. Finally, only the global
16 degree of crystallinity of the polymer is accounted for in the
17 thermodynamic model. Strictly speaking, also tie molecules
18 linking the crystalline lamellae can influence the solubility of
19 different species in the amorphous phase.^[26]

20 Due to the lack of solubility data, the following more critical
21 assumptions are considered:

- 22 A1. *Additive effect*: The quaternary system is approximated by a
23 ternary system: ethylene/(ICA+comonomer)/LLDPE, as sug-
24 gested by Alves et al.^[21] Thus, a “pseudo” component, repre-
25 senting the mixture of ICA plus comonomer, is defined for
26 which the thermodynamic parameters are identified. In this
27 assumption, no interaction between ICA and comonomer is
28 considered, which means that these species behave independ-
29 ently from each other as if they were present in a ternary
30 system (PE, ethylene, and either ICA or comonomer). This
31 is not unreasonable if the comonomer and ICA are similar
32 in structure. This assumption is thus applicable for the two
33 systems studied in this work, i.e., the comonomer 1-hexene
34 and *n*-hexane as ICA, as well as the comonomer 1-butene and
35 iso-butane as ICA. However, this assumption does not mean
36 that the ICA and the comonomer have the same solubility or
37 cosolubility effect, as discussed in the following two sections.
- 38 A2. *Polynomial approximations*: In order to reduce the computa-
39 tion time, the results from the SL EoS or the experimental
40 results, are approximated by polynomials of degree 1 or 2, as
41 suggested by Alves et al.^[21] Different pathways were consid-
42 ered for the two systems investigated in the present work, as
43 described in the following sections.

44 2.1.1. Polyethylene, in Presence of Ethylene, 1-Hexene, 45 and the ICA *n*-Hexane

46 For the first system, the comonomer 1-hexene and the ICA
47 *n*-hexane, both the comonomer and the ICA were found to have
48 comparable solubilities in a binary system, especially at low
49 pressure, as shown by **Figure 1** (Yao et al.^[27] and Jin et al.^[28]).
50 Therefore, Alizadeh et al.^[23] assumed it safe to consider that
51 they have similar solubility in LLDPE in a ternary or quater-
52 nary system. A similar observation was found for other three
53 and six carbon pairs, such as the isomers propene and propane,
54 where the difference in their solubility constant of Henry’s law
55 was 10% at 25 °C, as reported by Michaels et al.^[24] This can be
56 explained by the fact that 1-hexene and *n*-hexane have similar



19
20 **Figure 1.** Solubility of *n*-hexane and 1-hexene in LLDPE (binary systems)
21 at 70 °C (data from Yao et al.^[27] and Jin et al.^[28]).

22 shapes and same number of carbons, so almost the same size,
23 therefore, they have similar tendency to condense (i.e., same
24 volatility). Besides, they have similar nature of interaction with
25 LLDPE segments (i.e., same nature of van der Waals forces).^[23]
26 Therefore, in a quaternary system, the ratio of solubility of
27 1-hexene in LLDPE to *n*-hexane is assumed $r = \frac{S_{1-hexene}}{S_{n-hexane}} = 1$. Note
28 that for the second system, the comonomer 1-butene and the
29 ICA iso-butane, their binary solubilities in LLDPE are different,
30 and was accounted for as explained in Section 2.1.2.

31 For this system, copolymerization of ethylene with 1-hexene
32 in presence of the ICA *n*-hexane, solubility data are available
33 only for the ternary system ethylene/*n*-hexane/PE at 10 bar eth-
34 ylene^[27] (**Figure 2**). To use these data in a quaternary system
35 (Assumption A1: *Additive effect*), the ICA *n*-hexane is assumed
36 to thermodynamically behave like the comonomer 1-hexene (as
37 explained in the previous section).^[23]

38 The available ternary data of solubility (Figure 2) is then used
39 to obtain linear or polynomial equations (Assumption A2: *Poly-
40 nomial approximations*). It can be noticed that the solubility of
41 ethylene varies linearly over a small range with the pressure of
42 ICA/comonomer, therefore a polynomial of degree 1 could fit
43 the experimental data, while the solubility of comonomer varies
44 nonlinearly with its pressure, therefore a polynomial of degree
45 2 was necessary, as follows

$$46 \quad [M_1^p] = A(P_{ICA} + P_2) + B \quad (1)$$

$$47 \quad [M_2^p] = r \frac{P_2}{P_2 + P_{ICA}} [C(P_{ICA} + P_2)^2 + D(P_{ICA} + P_2)] \quad (2)$$

48 where $[M_i^p]$ and P_i are, respectively, the concentration in amor-
49 phous polymer (mol m^{-3}) and pressure (bar) of component
50 i (1 for ethylene and 2 for the comonomer) and r represents
51 the ratio of solubility of comonomer to ICA, which is equal to
52 one in this system. The values of the coefficients (A , B , C , D)
53 in Equations (1) and (2) are given in **Table 1**. It is important

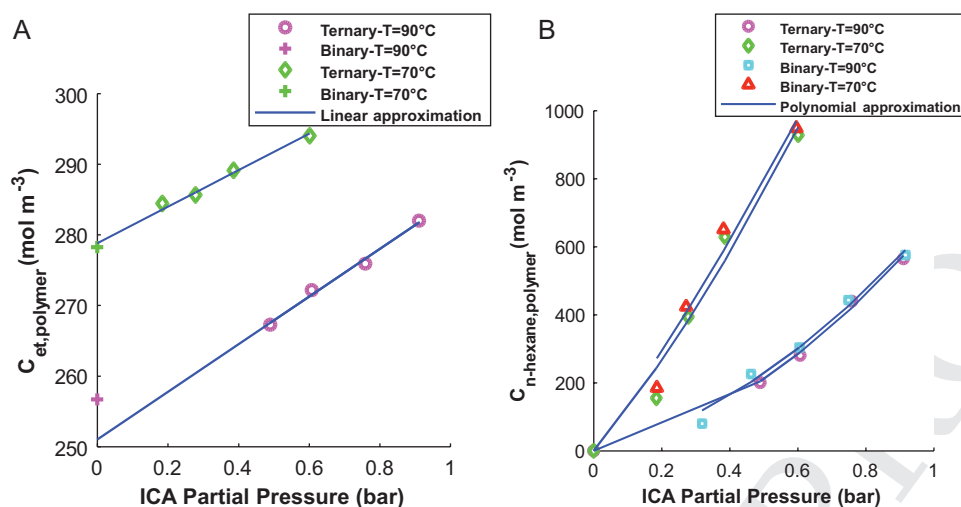


Figure 2. Ternary solubility data ethylene/*n*-hexane/LLDPE at 90 and 70 °C at 10 bar of ethylene (experimental data are taken for ternary systems from Yao et al.^[31] and for binary systems from Yao et al.^[27]): a) Concentration of ethylene in amorphous LLDPE as a function of the partial pressure of *n*-hexane, and b) concentration of *n*-hexane as a function of its partial pressure.

to mention that these coefficients are valid for the specific conditions (temperature and pressure) for which they were developed (i.e., ethylene pressure of 10 bars and pseudo-component “ICA+comonomer” pressure of 0 to 1 bar). It is also important to note that the concentration of ethylene only varies slightly as a function of the partial pressure of “*n*-hexane + 1-hexene,” however the concentration of *n*-hexane (and so of 1-hexene) is very sensitive to the partial pressure of the pseudo-component “ICA+comonomer,” which is necessary to account for in the model (Figure 2). Note that when increasing temperature, the slope of the concentration of *n*-hexane with its partial pressure decreases (from $C \approx 624$ to $506 \text{ mol m}^{-3} \text{ Pa}^{-2}$), while the slope of the concentration of ethylene increases (from $A \approx 34$ to $279 \text{ mol m}^{-3} \text{ Pa}^{-1}$). Increasing the temperature thus increases slightly the impact of ICA on ethylene absorption, but it remains very low. Besides, the figure shows that the concentration of *n*-hexane in amorphous PE increases slightly in a binary system compared to a ternary system. This was expected given the antisolvent effect of ethylene on ICA in a ternary system.^[29,30] Note that the concentration plots presented in this paper were calculated by converting solubility data (in g g^{-1} amorphous polymer) found in the open literature into mol m^{-3} using the amorphous polymer densities (i.e., the values of the swollen polymer density with different ICAs) estimated by Sanchez-Lacombe EoS for each case.

Table 1. Coefficients of the correlations allowing to estimate the ethylene and 1-hexene concentrations in amorphous LLDPE at 90 and 70 °C (valid at ethylene pressure of 10 bar and pseudo-component pressure on the range 0–1 bar).

	Value at 90 °C	Value at 70 °C	Units
A	33.8	25.9	$\text{mol m}^{-3} \text{ Pa}^{-1}$
B	251	278.8	mol m^{-3}
C	505.8	623.9	$\text{mol m}^{-3} \text{ Pa}^{-2}$
D	169.2	1206.3	$\text{mol m}^{-3} \text{ Pa}^{-1}$
<i>r</i>	1	1	–

Equations (1) and (2), with their identified parameters in Table 1, allow for the estimation of the concentration of ethylene and 1-hexene in the quaternary system ethylene/1-hexene/*n*-hexane/LLDPE at equilibrium. This information is all what is required for the rest of the paper regarding this system, and there is no need for the SL EoS here.

2.1.2. Polyethylene, in Presence of Ethylene, 1-Butene, and Iso-Butane as ICA

For the copolymerization of ethylene with 1-butene in presence of iso-butane as ICA, ternary data are not available for either ethylene/iso-butane/LLDPE or for ethylene/1-butene/LLDPE. Moreover, the available binary sorption data (Figure 3)^[32,33] indicate that 1-butene and iso-butane have different solubilities in the polymer and cannot be assumed to be similar, as could be done for 1-butene/*n*-butane and 1-hexene/*n*-hexane. Indeed, the solubility of 1-butene in HDPE is higher than that of iso-butane by almost a factor of $r = \frac{S_{1\text{-butene}}}{S_{\text{iso-butane}}} = 1.78$, at nearly the same temperature.

Due to this lack of data, the following assumptions are made only for this system:

- A3. The ratio of sorption of 1-butene to iso-butane, *r* (Figure 3), identified in a binary system, was assumed to remain unchanged in a ternary system, and to remain unchanged within a temperature range of 65–90 °C. This means that they are assumed to have the same cosolubility effect on ethylene.
- A4. The k_{ij} parameters are assumed to vary linearly with temperature. So, as solubility data are not available, an extrapolation of k_{ij} is done to predict them at 90 °C.
- A5. The solubility of iso-butane in HDPE and LLDPE is assumed to be the same, as only solubility data in HDPE are available (in a binary system^[32]).

Again, Assumption A1 is applied to this system: The comonomer and ICA were assumed to have an additive effect in a

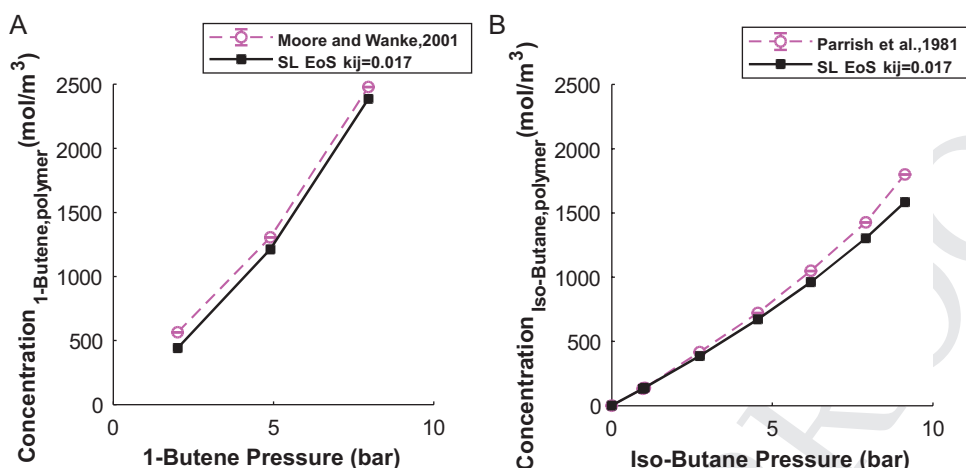


Figure 3. a,b) Binary solubility data in HDPE of comonomer 1-butene at 68.9 °C, and ICA iso-butane at 65.6 °C.

quaternary system. Alves et al.^[21] validated this assumption for propane and iso-butane based on reaction data from patents. This means that propane and iso-butane do not affect the solubility of each other (i.e., there is no cosolubility effect), which is reasonable in view of their similarities. A similar assumption can be done regarding 1-butene and iso-butane in our system. Based on this assumption, Alves et al.^[21] estimated the binary interaction parameters k_{ij} for the ternary system ethylene/iso-butane/LLDPE by fitting to experimental solubility data of the binary systems ethylene/LLDPE and iso-butane/HDPE at 70 °C (Table 2).^[32] Thus, the correlation between the ICA and the comonomer becomes (combining Assumptions A1, A2, and A3)

$$[M_2^e] = r \frac{P_2}{P_2 + P_{ICA}} [E(P_{ICA} + P_2) + F] \quad (3)$$

In order to identify the parameters of Equations (1) and (3) for the quaternary system, SL EoS is first used in the ternary system ethylene/iso-butane/LLDPE (with k_{ij} identified using binary solubility data^[21]) to identify the solubility of ethylene and iso-butane at different pressures of iso-butane. Then, the k_{ij} parameters were extrapolated over temperature to have values at 90 °C (Assumption A4) (Figure 4, Table 3). The concentration of 1-butene is then calculated using $S_{1-butene} = r S_{iso-butane}$. From the obtained data points, polynomials of order 1 were identified for both ternary systems.

As in the first system, it can be noted that the concentration of ethylene only varies slightly as a function of the partial pressure of the pseudo-component “isobutane+1-butene,” while the concentration of comonomer 1-butene is very sensitive to its partial pressure (Figure 4).

Table 2. Binary interaction parameters of the ternary system ethylene/iso-butane/LLDPE (based on binary thermodynamic data).

Temperature [°C]	Ethylene/iso-butane (k_{12})	Ethylene/LLDPE (k_{13}) ^[23]	Iso-butane/LLDPE (k_{23})
70	0	-0.014	0.025 (74 °C) ^[21]
80	0	-0.022	0.022 (82 °C) ^[21]
90	0	-0.032	$-3.75 \times 10^{-4}T (K) + 0.1551$

2.2. Kinetic Model

A classical reaction scheme (Table 4) of copolymerization of ethylene in presence of a catalyst having one type of active sites was considered (see, for instance, de Carvalho et al.^[34] McAuley et al.^[35] Chatzidoukas et al.^[15]). The only difference between the two copolymerization systems, with the comonomer 1-hexene or with 1-butene, is the values of the rate constants.

The following notations are used in Table 4: S_p : potential catalyst active sites, P_0 : activated vacant catalyst sites, P_* : total active sites (vacant P_0 and occupied by a polymer chain $P_{n,i}$), $P_{n,i}$: living copolymer chains of length n ending with monomer i , D_n : dead copolymer chains of length n , and C_d : deactivated catalyst sites.

The reaction rates resulting from the proposed reaction scheme are given in Table 5. All concentrations are in (mol m^{-3}) and the following notations are used: λ_k moment k of living chains, μ_k moment k of dead chains, and M_w is the instantaneous polymer average molecular weight.

The values of the different kinetic rate constants are given in Tables 6 and 7. E refers to the activation energy and k_0 to the pre-exponential factor. For the case of ethylene-co-1-butene, the parameters were taken from Chatzidoukas et al.^[15] or Ghasem et al.^[37] For the system ethylene-co-1-hexene in gas phase, fewer parameters are available. Chakravarti et al.^[38] gave some kinetic parameters for this system using a metallocene catalyst. In order to keep both systems comparable in terms of catalyst activity, only the reactivity ratios were taken from Chakravarti et al.,^[38] and the other parameters and ratios were kept as for the first system. The identification of a specific kinetic model for a defined system is out of the scope of this work as our

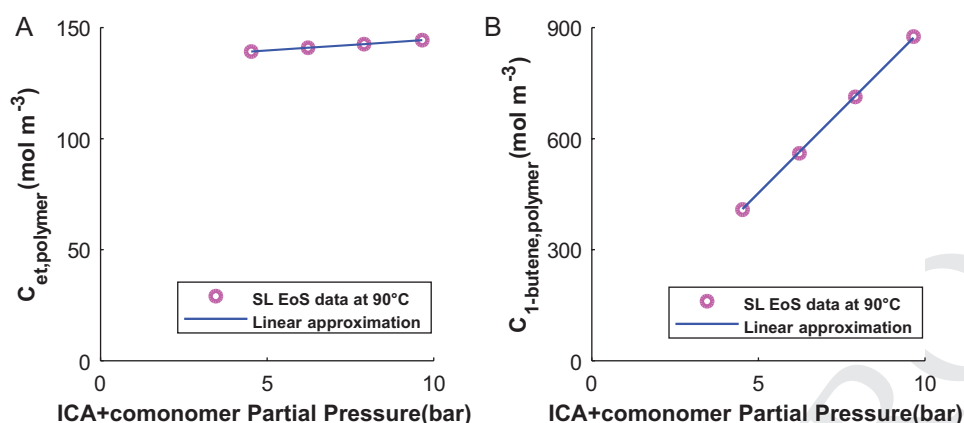


Figure 4. Concentrations in amorphous LLDPE obtained using SL EoS, pseudo-quaternary system ethylene/(ICA+comonomer)/HDPE, at 90 °C (after extrapolation of k_{ij}) and 7 bar of ethylene: a) ethylene and b) comonomer 1-butene.

primary focus is to explore the impact of the cosolubility effect on grade change optimization.

2.3. Fluidized Bed Reactor Model

The FBR is modeled as a single-phase CSTR. This assumption is a reasonable initial approximation in industrial FBR given its high recycle ratio and low single pass conversion.^[8,35] Fresh or prepolymerized catalyst particles, gas species (monomers, N_2 , H_2) and condensed gas (ICA) are assumed to be fed continuously at the bottom of the reactor. Thus, the FBR can roughly be divided into two compartments: one super-dry compartment in the containing only gas and polymer, and one much smaller compartment in the bottom also containing condensed vapors. Only the upper compartment is considered in the present model, which represents most of the reactor volume. Indeed, when operating under condensed mode, the injected liquid species evaporate rapidly and the major part of the reactor only contains solid and gas species (i.e., super-dry mode).^[39]

The mass balances of the different species in the FBR are given in **Table 8**, with the following notations, ε_{bed} : porosity of the bed, X_i and $X_{i,in}$: mass fractions of component i in the recycle and the input stream, respectively, $h(m)$: bed height, $V_{bed}(m^3)$: bed volume, $A(m^2)$: cross-sectional area of the bed

Table 3. Coefficients of the correlations allowing to estimate the ethylene and 1-butene concentrations in amorphous LLDPE at 90 °C (valid at ethylene pressure of 7 bar and pseudo-component pressure on the range 5–10 bar).

Parameter	At 90 °C	Units
A	0.992	$\text{mol m}^{-3} \text{Pa}^{-1}$
B	134.73	mol m^{-3}
E	90.209	$\text{mol m}^{-3} \text{Pa}^{-1}$
F	1.0826	mol m^{-3}
r	1.78	-

Q_0 ($\text{m}^3 \text{s}^{-1}$): bed outlet volumetric flow rate, F_k (kg s^{-1}) inlet flow rate of component k , F_{rec} (kg s^{-1}) recycling flow rate, and X_k mass fraction of component k in the gas phase.

The mass balance for the bed height is given by

$$\frac{dh}{dt} = (R_{M_1} M_{w1} + R_{M_2} M_{w2}) \frac{V_{bed}}{\rho_p A} + \frac{F_{cat} - Q_0}{(1 - \varepsilon_{bed}) \rho_{cat} A} \quad (4)$$

And the steady-state mass balance for the polymer in the bed is given by the following equation^[40]

$$Q_0 = \frac{V_{bed} (R_{M_1} M_{w1} + R_{M_2} M_{w2}) (1 - \varepsilon_{bed})}{(1 - \varepsilon_{bed}) \rho_p + \varepsilon_{bed} (M_1 M_{w1} + M_2 M_{w2})} \quad (5)$$

where ρ_p and ρ_{cat} are the densities of the polymer (around 920 kg m^{-3}) and catalyst (2800 kg m^{-3}), respectively. The dimensions of the bed are given in **Table 9**.

Table 4. Kinetic scheme of the copolymerization of ethylene with a catalyst of one site (without cocatalyst).

Designation	Reaction
Spontaneous activation	$S_p \xrightarrow{k_s} P_0$
Chain initiation	$P_0 + M_i \xrightarrow{k_{oi}} P_{1,i}$
Propagation	$P_{n,i} + M_j \xrightarrow{k_{pj}} P_{n+1,j}$
Spontaneous deactivation	$P_{n,i} \xrightarrow{k_{sp}} C_d + D_n, P_0 \xrightarrow{k_{sp}} C_d$
Spontaneous chain transfer	$P_{n,i} \xrightarrow{k_{sp}} P_0 + D_n$
Chain transfer to hydrogen (H_2)	$P_{n,i} + H_2 \xrightarrow{k_{sh}} P_0 + D_n$
Chain transfer to monomer M_j	$P_{n,i} + M_j \xrightarrow{k_{mj}} P_{1,j} + D_n$

Table 5. Reaction rates of the different species ($\text{mol m}^{-3} \text{s}^{-1}$).

$$R_{S_p} = -k_a[S_p]$$

$$R_{P_0} = k_a[S_p] - k_{d_{sp}}[P_0] - (k_{01}[M_1^p] + k_{02}[M_2^p])[P_0] + (k_{t_{sp}} + k_{tH}[H_2^p])\lambda_0$$

$$R_{\lambda_0} = [P_0](k_{01}[M_1^p] + k_{02}[M_2^p]) - \lambda_0(k_{d_{sp}} + k_{t_{sp}} + k_{tH}[H_2^p])$$

$$R_{\lambda_1} = [P_0](k_{01}[M_1^p] + k_{02}[M_2^p]) + \lambda_0((k_{tm11}\phi_1 + k_{tm21}\phi_2 + k_{p11}\phi_1 + k_{p21}\phi_2[M_1^p] + (k_{tm12}\phi_1 + k_{tm22}\phi_2 + k_{p12}\phi_1 + k_{p22}\phi_2)[M_2^p]) - \lambda_1((k_{d_{sp}} + k_{t_{sp}} + k_{tH}[H_2^p]) + (k_{tm11}\phi_1 + k_{tm21}\phi_2)[M_1^p] + (k_{tm12}\phi_1 + k_{tm22}\phi_2)[M_2^p])$$

$$R_{\lambda_2} = [P_0](k_{01}[M_1^p] + k_{02}[M_2^p]) + \lambda_0((k_{tm11}\phi_1 + k_{tm21}\phi_2)[M_1^p] + (k_{tm12}\phi_1 + k_{tm22}\phi_2)[M_2^p]) + (\lambda_0 + 2\lambda_1)((k_{p11}\phi_1 + k_{p21}\phi_2)[M_1^p] + (k_{p12}\phi_1 + k_{p22}\phi_2)[M_2^p]) - \lambda_2(k_{d_{sp}} + k_{t_{sp}} + k_{tH}[H_2^p]) + (k_{tm11}\phi_1 + k_{tm21}\phi_2)[M_1^p] + (k_{tm12}\phi_1 + k_{tm22}\phi_2)[M_2^p]$$

$$R_{M_0} = \lambda_0(k_{d_{sp}} + k_{t_{sp}} + k_{tH}[H_2^p] + (k_{tm11}\phi_1 + k_{tm21}\phi_2)[M_1^p] + (k_{tm12}\phi_1 + k_{tm22}\phi_2)[M_2^p])$$

$$R_{M_1} = \lambda_1(k_{d_{sp}} + k_{t_{sp}} + k_{tH}[H_2^p] + (k_{tm11}\phi_1 + k_{tm21}\phi_2)[M_1^p] + (k_{tm12}\phi_1 + k_{tm22}\phi_2)[M_2^p])$$

$$R_{M_2} = \lambda_2(k_{d_{sp}} + k_{t_{sp}} + k_{tH}[H_2^p] + (k_{tm11}\phi_1 + k_{tm21}\phi_2)[M_1^p] + (k_{tm12}\phi_1 + k_{tm22}\phi_2)[M_2^p])$$

$$R_{H_2} = k_{tH}[H_2^p]\lambda_0$$

$$R_{M_1} = (k_{01}[P_0] + (k_{tm11}\phi_1 + k_{tm21}\phi_2 + k_{p11}\phi_1 + k_{p21}\phi_2)\lambda_0)[M_1^p]$$

$$R_{M_2} = (k_{02}[P_0] + (k_{tm22}\phi_2 + k_{tm12}\phi_1 + k_{p22}\phi_2 + k_{p12}\phi_1)\lambda_0)[M_2^p]$$

With $\phi_1 = \frac{k_{p21}[M_1^p]}{k_{p12}[M_2^p] + k_{p21}[M_1^p]}$, $\phi_2 = 1 - \phi_1$,

$$[H_2^p] (\text{mol m}^{-3} \text{ am. polymer}) = S_{H_2} \frac{\rho_{PE}}{MW_{H_2}}, S_{H_2} (\text{g H}_2 \text{ g}^{-1} \text{ am. polymer}) = 10^{-9} P_{H_2}^{[36]}$$

$$\lambda_k = \lambda_{k,1} + \lambda_{k,2} = \sum_{n=1}^{\infty} n^k [P_{n,1}] + \sum_{n=1}^{\infty} n^k [P_{n,2}]$$

$$\mu_k = \sum_{n=2}^{\infty} n^k [D_n]$$

$$M_w = \bar{M}_w \frac{(\lambda_2 + \mu_2)}{(\lambda_1 + \mu_1)}, \text{ with } \bar{M}_w = \sum_{i=1}^2 \varphi_i M_{wi}, \varphi_i = \frac{R_{M_i}}{\sum_{i=1}^2 R_{M_i}}$$

2.4. Correlations of Key Properties

The main properties to be controlled in the gas-phase copolymerization of ethylene are the melt index (MI, or melt flow index MFI, g/10 min) and the polymer density (ρ_{pol}). Correlations are therefore needed to estimate these properties. The available correlations in the literature can be divided into two categories:

A. Correlations which relate the final properties to the individual monomer conversions in the reactor (i.e., to reacted species) (Table 10).^[11] These correlations are universal and remain valid when varying the operating conditions.

Table 6. Pre-exponential factors and activation energies of the kinetic parameters of copolymerization of ethylene and a comonomer (common values for both systems) ($k_i = k_{i,0} e^{-\frac{E_a}{RT}}$).

Parameter	Value
Spontaneous activation ^[37]	
$k_{a,0}$ [s^{-1}]	7.2×10^4
E_a [J mol^{-1}]	33 472
Spontaneous deactivation ^[15]	
$k_{d_{sp},0}$ [s^{-1}]	7.2
$E_{d_{sp}}$ [J mol^{-1}]	33 472
Initiation ^[37]	
$k_{0,1}$ [$\text{m}^3 \text{mol}^{-1} \text{s}^{-1}$]	2.9×10^2
$E_{0,1}$ [J mol^{-1}]	37 656
Spontaneous chain transfer ^[15]	
$k_{t_{sp},0}$ [$\text{m}^3 \text{mol}^{-1} \text{s}^{-1}$]	7.2
$E_{t_{sp}}$ [J mol^{-1}]	33 472
Transfer to hydrogen ^[37]	
$k_{tH,0}$ [$\text{m}^3 \text{mol}^{-1} \text{s}^{-1}$]	6.3
E_{tH} [J mol^{-1}]	33 472
Transfer to monomer ^[37]	
$k_{tm11,0}$ [$\text{m}^3 \text{mol}^{-1} \text{s}^{-1}$]	0.15
$k_{tm12,0}$ [$\text{m}^3 \text{mol}^{-1} \text{s}^{-1}$]	0.43
$k_{tm21,0}$ [$\text{m}^3 \text{mol}^{-1} \text{s}^{-1}$]	0.15
$k_{tm22,0}$ [$\text{m}^3 \text{mol}^{-1} \text{s}^{-1}$]	0.43
$E_{tmij,0}$ [J mol^{-1}]	33 472
Activation energy of propagation ^[15]	
E_{pij} [J mol^{-1}]	37 656

B. Correlations which relate the final properties to the operating conditions (i.e., T , P , or concentrations of unreacted species in the gas phase), such as^[11]

Table 7. Propagation rate coefficients of the copolymerization of ethylene with a comonomer.

	1-Butene	1-Hexene
Reactivity ratios (-):		
$r_1 = k_{p11}/k_{p12}$	42.5	18.94 ^[38]
$r_2 = k_{p22}/k_{p21}$	0.023	0.04 ^[38]
Pre-exponential factor of propagation [$\text{m}^3 \text{mol}^{-1} \text{s}^{-1}$]:		
$k_{p11,0}$	2.48×10^4 ^[37]	2.48×10^4
$k_{p12,0}$	5.82×10^2 ^[37]	$k_{p11}/r_1 = 1.3 \times 10^3$
$k_{p21,0}$	1.86×10^4 ^[37]	$k_{p22}/r_2 = 2.65 \times 10^3$
$k_{p22,0}$	4.37×10^2	$1.06 \times 10^{2a)}$, ^[38]
Comonomer initiation [$\text{m}^3 \text{mol}^{-1} \text{s}^{-1}$]:		
$k_{0,2}$	40.7 ^[37]	$k_{0,1}k_{p22}/k_{p11} = 1.25$
$E_{0,2}$ [J mol^{-1}]	37 656	37 656

^{a)} Calculated with respect to the ratio k_{p11}/k_{p22} in ref. [38].

Table 8. Mass balances of the different species in the FBR.

Monomer i	$\frac{d[M_i]}{dt} = \frac{F_i - F_{rec} X_{M_i}}{M_{w,i} \epsilon_{bed} V_{bed}} - \frac{Q_0 [M_i]}{\epsilon_{bed} V_{bed}} - \frac{(1 - \epsilon_{bed}) R_{M_i}}{\epsilon_{bed}} - \frac{[M_i] A}{V_{bed}} \frac{dh}{dt}$
Hydrogen	$\frac{d[H_2]}{dt} = \frac{F_{H_2} - F_{rec} X_{H_2}}{M_{w,H_2} \epsilon_{bed} V_{bed}} - \frac{Q_0 [H_2]}{\epsilon_{bed} V_{bed}} - \frac{(1 - \epsilon_{bed}) R_{H_2}}{\epsilon_{bed}} - \frac{[H_2] A}{V_{bed}} \frac{dh}{dt}$
Nitrogen	$\frac{d[N_2]}{dt} = \frac{F_{N_2} - F_{rec} X_{N_2}}{M_{w,N_2} \epsilon_{bed} V_{bed}} - \frac{Q_0 [N_2]}{\epsilon_{bed} V_{bed}} - \frac{[N_2] A}{V_{bed}} \frac{dh}{dt}$
ICA	$\frac{d[I_{CA}]}{dt} = \frac{F_{ICA} - F_{rec} X_{ICA}}{M_{w,ICA} \epsilon_{bed} V_{bed}} - \frac{Q_0 [I_{CA}]}{\epsilon_{bed} V_{bed}} - \frac{[I_{CA}] A}{V_{bed}} \frac{dh}{dt}$
Potential catalyst sites S_p	$\frac{d[S_p]}{dt} = \frac{F_{cat} [S_{p,in}]}{\rho_{cat} (1 - \epsilon_{bed}) V_{bed}} - \frac{Q_0 [S_p]}{(1 - \epsilon_{bed}) \epsilon_{bed} V_{bed}} + R_{S_p} - \frac{[S_p] A}{V_{bed}} \frac{dh}{dt}$
$Y: P_0, \lambda_0, \lambda_1, \lambda_2, \mu_0, \mu_1, \mu_2$	$\frac{d[Y]}{dt} = R_Y - \frac{Q_0 [Y]}{(1 - \epsilon_{bed}) \epsilon_{bed} V_{bed}} - \frac{[Y] A}{V_{bed}} \frac{dh}{dt}$

$$\ln MI_i = 3.5 \ln \left(k_0 + k_1 \frac{[M_2]}{[M_1]} + k_2 \frac{[M_3]}{[M_1]} + k_3 \frac{[H_2]}{[M_1]} \right) + k_4 \left(\frac{1}{T} - \frac{1}{T_0} \right)$$

$$\rho_i = \rho_0 + \rho_1 \ln MI_i - \left[\rho_2 \frac{[M_2]}{[M_1]} + \rho_3 \frac{[M_3]}{[M_1]} \right]^{\rho_4}$$

(6)

where $k_{i(i=1-4)}$, $\rho_{k(k=0-3)}$ are tuning parameters and M_2 and M_3 are comonomers. Other correlations also exist in the open literature.^[14,41-44] Such correlations are only valid for the set of operating conditions for which they were derived and cannot be used to account for thermodynamic effects such as the cosolubility effect. Therefore, such correlations are not valid during grade transition where the operating conditions change.

In this work, the correlations of the first category will be employed (Table 10), as only such correlations would be able to account for the cosolubility effect, for instance. In this work, the correlations developed by McAuley and MacGregor^[11] for both MI and density are used (see Table 10).

The derivation of these correlations is based on physical interpretations. For instance, the melt index is highly correlated to the polymer molecular weight distribution and branching characteristics.^[45] To simplify, the instantaneous melt index is usually correlated to the instantaneous average polymer molecular weight M_w . The molecular weight is in turn affected by the concentration of monomer, comonomer, and hydrogen. More particularly, hydrogen plays the role of a chain transfer agent in catalytic ethylene reactions, thus allowing to reduce the

Table 9. Reactor dimensions.

Parameter	Designation	Value
D_{bed}	Bed diameter	4.75 m
ϵ_{bed}	Bed voidage	0.7
H	Height of the bed	13.3 m

polymer molecular weight.^[46] It constitutes therefore a primary manipulated variable during grade transitions. The melt index considered in this work represents the flow rate of a molten polymer under the load of 2.16 kg at 190 °C (ASTM D1238).^[47,26]

Concerning the polymer density, it is strongly affected by the length and the number of short chain branches. Hence, it is mainly governed by the fraction of reacted comonomer in the copolymer (C_x) (Table 10).^[48] By creating short chain branches on the polymer, the comonomer allows reducing the polymer density. As a consequence, the crystallinity of the polymer also decreases.^[26] The comonomer constitutes the second important manipulated variable during grade transition. The correlation proposed by McAuley and MacGregor^[11] is based on patent data collected by Sinclair,^[49] and it relates the instantaneous polymer density to the comonomer incorporation in the polymer by including C_x (where $C_x = \phi_2 \times 100$, and $\phi_2 = \frac{R_{M_2}}{R_{M_2} + R_{M_1}}$, see Table 5).

The cumulative properties (of the polymer exiting the reactor) can be calculated from the instantaneous ones (those being produced at time t) by integration over the residence time (τ). Therefore, the cumulative melt index (MI_c) becomes^[54]

$$\frac{d(MI_c^{-0.286})}{dt} = \frac{1}{\tau} MI_i^{-0.286} - \frac{1}{\tau} MI_c^{-0.286}$$

(7)

Similarly, the cumulative density of the polymer (ρ_c) is given by^[8]

$$\frac{d(\rho_c^{-1})}{dt} = \frac{1}{\tau} \rho_i^{-1} - \frac{1}{\tau} \rho_c^{-1}$$

(8)

3. Grade Transition Strategy

Dynamic optimization is employed to optimize the transition between different grades of LLDPE in the FBR using the combined kinetic and thermodynamic model.

3.1. Formulation of the Optimization Problem

The manipulated variables are the flow rates of hydrogen and comonomer and the controlled outputs are the melt index and the polymer density.

The optimization problem can be written as follows^[12]

Table 10. Correlations of Category A for the properties of the polymer: MI and density.

Ref.	Melt index [g/10 min]	Density [g cm ⁻³]	Data from
[11]	$M_w = 111525 MI_i^{-0.288}$ (or $MI_i = 3.35 \times 10^{17} M_w^{-3.47}$)	$\rho_i = 0.966 - 0.02386 C_x^{0.514}$	Butene grades ^[49]
[50]	$MI_i = 2.7 \times 10^{19} M_w^{-3.92}$		[51]
[51]	$MI_i = 4.195 \times 10^{19} M_w^{-3.92}$		
[48]	$MI_i = 3 \times 10^{19} M_w^{-3.92}$	$\rho_i = -0.023 \ln C_x + 0.9192$	Octene grades ^[53]

$$\min_{u(t)} J(u(t), x(t)), t \in [t_0, t_f] \quad (9)$$

$$u_{\min} \leq u(t) \leq u_{\max} \quad (10)$$

where J is the objective function, $x(t)$ is the vector of state variables (see Table 8), and $u(t)$ represents the vector of manipulated variables, $u(t) = [F_{H_2}, F_{\text{com}}]$. The inequality constraints (10) indicate the available ranges of manipulated variables.

3.2. Objective Function

The considered objective function is the following

$$J(u) = \int_{t_0}^{t_f} w_1 \frac{|MI_i - MI_{sp}|}{MI_{sp}} + w_2 \frac{|MI_c - MI_{sp}|}{MI_{sp}} + w_3 \frac{|\rho_i - \rho_{sp}|}{\rho_{sp}} + w_4 \frac{|\rho_c - \rho_{sp}|}{\rho_{sp}} dt + w_5 \sum_{i=1}^2 \frac{\Delta u_i}{u_i(t_0)} \quad (11)$$

By considering both instantaneous and cumulative properties (of the melt index and polymer density), and by a good tuning the weighting factors w_i (with $i = 1 - 5$), one may accelerate the convergence of cumulative properties while keeping the instantaneous properties within an acceptable range. The last term on the right hand side of this equation is also intended to minimize the variation of the input during the transition, in order to avoid oscillations (as in model predictive control). The normalization of the different terms (i.e., the division by the set-points of the MI and density) allows for an easier tuning of the weighting factors. The indices i , c , and sp refer to the instantaneous, cumulative, and set-point properties, respectively.

At a constant reaction rate, the proposed objective function allows reducing the quantity of transition product as well as the transition time, even though the time is not explicitly minimized in this function. If the reaction rate varies during the transition, then this objective function allows minimizing only the transition time. The minimization of the transition product would necessitate, in case of variable reaction rate, to multiply the criterion by the instantaneous reaction rate (R_p), as done by McAuley and MacGregor,^[12] for instance. Takeda et al.^[13] suggested that the choice between minimizing the transition product and the transition time should be based on the market demand: where at high polymer sales and plant capacity production it is preferred to minimize the transition time; while at low polymer sales and reduced plant capacity it is preferred to minimize the transition production and authorize a longer transition time. A transition product can usually be sold, although at a discounted price.

3.3. Degrees of Freedom of the Inputs

It is usually sufficient to assume the manipulated variables (here, the flow rates of hydrogen and comonomer) to vary by a series of ramps during the transition.^[12] Based on the literature study and the residence time of the FBR ($\approx 4-6$ h in this

Table 11. LLDPE grades considered in the grade transition policy.

Grade	Melt index target [g/10 min]		Density target [kg m ⁻³]	
	1-Hexene	1-Butene	1-Hexene	1-Butene
A	0.54	4.5	923	918.5
B	2	2	916	922
A	0.54	4.5	923	918.5

study, depending on the operating conditions), the transition is divided into five intervals, where the final interval corresponds to the steady-state interval, to maintain until the end of the production of the new grade. Thus, the optimization allows switching the flow rates every 2 h during the first 8 h, and the last ramp corresponds to the steady-state flow rate of the new grade.

4. Simulation Results and Discussion

The proposed strategy is evaluated in grade transition starting from grade A, to grade B with higher or lower MI and ρ , then coming back to grade A, for both of the copolymerization systems (Table 11). These choices are based on LLDPE specifications, i.e., $MI \in [0.01-100]$ g/10 min^[55] and $\rho \in [915-935]$ kg m⁻³.^[56] The duration of each grade production is usually defined by the market demand, the specifications or the claims of the production. Here, an arbitrary duration of production of each grade of 30 h is implemented in both systems. No particular change is required at the optimization level to change to shorter or longer production periods, only the final times need to be indicated. The initial steady-state conditions, producing grade A, are given in Table 12. This weighting factors were tuned as follows, except otherwise mentioned: $w_1 = 0.08$, $w_2 = 1$, $w_3 = 8$, $w_4 = 19$, and $w_5 = 10^4$. This choice was based on few simulation tests, in a way to ensure a compromise between fast convergence of the cumulative properties while reducing the overshoots of the instantaneous properties. Indeed, while allowing for big variations in the instantaneous properties leads to a faster convergence of the cumulative properties, some conditions of comonomer or hydrogen pressures might lead to polymer softening or sticking problems.^[3] In the following simulations, temperature control is assumed to be perfect in the bed, so that the working temperature is constant.

Table 12. Initial conditions of the grade transition simulations (leading to grade A under steady state).

	1-Hexene	1-Butene
T [°C]	90	90
P_1 [bar]	9.4	7
P_2 [bar]	0.35	1.55
P_{ICA} [bar]	0.6	3.5
P_{H_2} [bar]	2.2	2.2

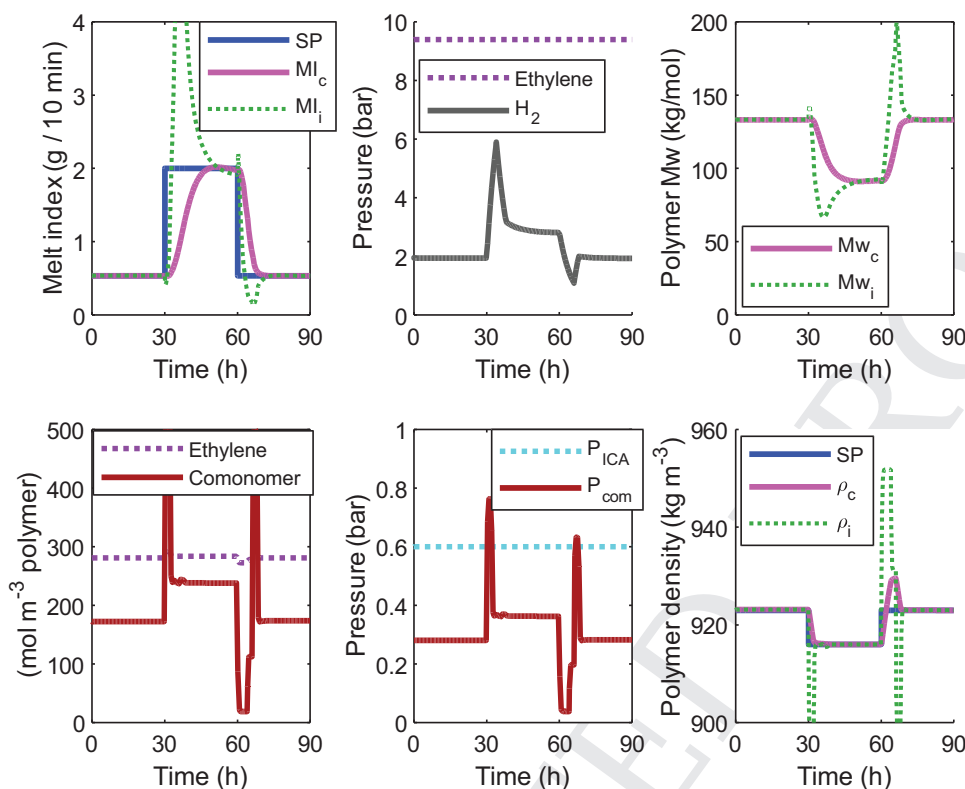


Figure 5. Grade transition in ethylene-1-hexene copolymerization in presence of *n*-hexane at 90 °C ($w_1 = 0.08$, $w_2 = 1$, $w_3 = 8$, $w_4 = 19$, $w_5 = 0$).

4.1. Copolymerization of Ethylene and 1-Hexene in Presence of *n*-Hexane as ICA

The optimization strategy was evaluated using the parameters of the first system, i.e., the copolymerization of ethylene with 1-hexene in presence of *n*-hexane. Note that the thermodynamic model was developed for this system for ethylene pressure of 10 bar and pseudo-component (i.e., comonomer plus ICA) pressure on the range of 0–1 bar. Therefore, the simulations (including the choices of the set-points) are conducted in a way to respect these ranges.

Figure 5 shows the results of the two grade transitions, from A to B, and from B back to A. This scenario was simulated using the following weighting factors: $w_1 = 0.08$, $w_2 = 1$, $w_3 = 8$, $w_4 = 19$, and $w_5 = 0$, therefore the instantaneous properties (MI_i and ρ_i) go beyond the SP during the transition in order to accelerate the convergence of the cumulative properties (MI_c and ρ_c). This is related to the variations of the flow rates of hydrogen and 1-hexene, which are higher at the beginning of the grade transition and then they stabilize, as indicated by the increase in the pressure. The overshoots in the instantaneous properties can be reduced by reducing the weighting factors multiplying the cumulative properties w_2 and w_4 compared to those of the instantaneous properties w_1 and w_3 , or by considering $w_5 \neq 0$, or by adding constraints on the outputs, as discussed in the following scenarios. The MI is inversely proportional to the polymer molecular weight. Therefore, an increase in the hydrogen pressure during the transition, from grade A to B, for instance, led to a decrease in the polymer molecular

weight and thus to an increase in the melt index. Likewise, an increase in the comonomer pressure during the transition from grade A to B, led to an increase in the amount of short branches and thus to a decrease in the polymer density. The proposed strategy allows to move either to higher (grade A to grade B) or lower (B to A) values of MI, and vice versa for ρ .

The figure shows that the concentration of ethylene in the polymer particles (which constitutes the site of the reaction) does not change significantly during the transition, where the comonomer flow rate is varied, so the cosolubility effect is negligible in this sense and under the realized changes in the comonomer pressure. Note that the ethylene pressure is maintained constant in all the grades. However, the concentration of comonomer in the polymer particles is highly affected by these changes, which demonstrates the necessity of a good thermodynamic model. The impact of the thermodynamic model is investigated more deeply in the last section. Note that the total pressure of comonomer and ICA reached 1.35 bar at the maximum in this simulation, but only for a short duration, and therefore the employed thermodynamic correlation remains valid during most of the time ($P_{ICA} + P_{com} = 0-1$ bar).

The same scenario presented in **Figure 5** was simulated while tracking only the cumulative properties (i.e., $w_1 = w_3 = 0$) and considering constraints on the instantaneous properties, as follows: $0.1 < MI_i < 3$ and $910 < \rho_i < 935$ (**Figure 6**). It can be seen that the convergence of the cumulative properties is slowed down compared to **Figure 5**, but the overshoots in the instantaneous properties (MI_i and ρ_i) are reduced and kept within the constraints. Adding hard constraints allows remaining within

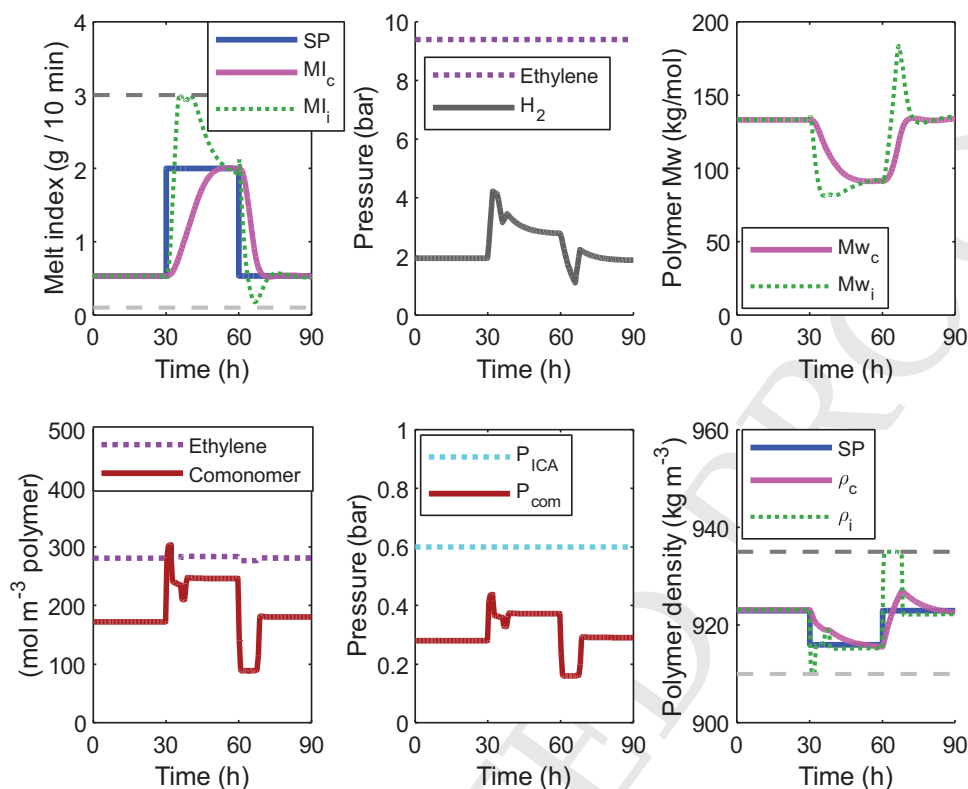


Figure 6. Grade transition in ethylene-1-hexene copolymerization in presence of *n*-hexane: Tracking of the cumulative properties ($w_1 = w_3 = w_5 = 0$, $w_2 = 1$, $w_4 = 4$), with constraints on the instantaneous properties ($0.1 < MI_i < 3$ and $910 < \rho_i < 935$).

the acceptable range of properties, but it slows down the calculation. Another way to reduce the overshoots in the instantaneous properties, without considering constraints, consists of increasing the values of w_2 and w_4 with respect to w_1 and w_3 or by considering $w_5 \neq 0$.

4.2. Copolymerization of Ethylene and 1-Butene in Presence of Iso-Butane as ICA

The proposed grade transition optimization strategy was evaluated in the second system: ethylene and 1-butene copolymerization in presence of iso-butane as ICA. Note that the thermodynamic model was developed for different conditions for this system, i.e., ethylene pressure of 7 bar and pseudo-component pressure on the range of 5–10 bars. The set-points of the melt index and polymer density of grades A and B were also set differently in this system, but still within LLDPE grades. The same weighting factors as the first system were considered.

Figure 7 shows the simulation results. The melt index converges in about 6 h to the set-point, while the density converges to the set-point in 2 h. The overshoots of the instantaneous properties remain acceptable, but they can be reduced by either manipulating the weighting coefficients (as discussed in the following scenario) or by adding hard constraints on the outputs as discussed in the previous section. Note that the total pressure of comonomer and ICA is around 5 bar, therefore

the employed thermodynamic correlation is valid ($P_{ICA} + P_{com} = 5\text{--}10$ bar).

The last term of the objective function ($w_5 \sum_{i=1}^2 \frac{\Delta u_i}{u_i(t_0)}$) can allow minimizing the variation of the manipulated variables (flow rates of hydrogen and the comonomer), and thus to reduce the overshoots in the instantaneous properties. Indeed, injecting big amounts of hydrogen or comonomer rapidly increases the risk of polymer softening and stickiness.^[3] As a consequence, adding this term is expected to reduce the overshoots in instantaneous properties. Due to the low values of the variations of the flow rates, it was necessary to have a high weighting factor, $w_5 = 10^4$, to ensure an impact on the performance. Figure 8 shows the results when adding this term to the objective function, which is to be compared to Figure 7 done under the same conditions but without this term. The figure clearly shows that the pressures of hydrogen and comonomer undergo less changes. As a consequence, the instantaneous properties have lower overshoots. However, this delays a little the convergence of the cumulative properties to the set-points. A compromise is thus to be determined between fast convergence of the cumulative properties and less variation in the instantaneous properties.

In order to evaluate the gain realized by the optimization strategy, its performance was compared to the case of injecting the optimal feed rates of the final grade during the transition (here called the final SS), as done, for instance, by Rahimpour et al.^[8] (Figure 9). When employing a constant flow rate during the transition, the convergence time is that of the residence

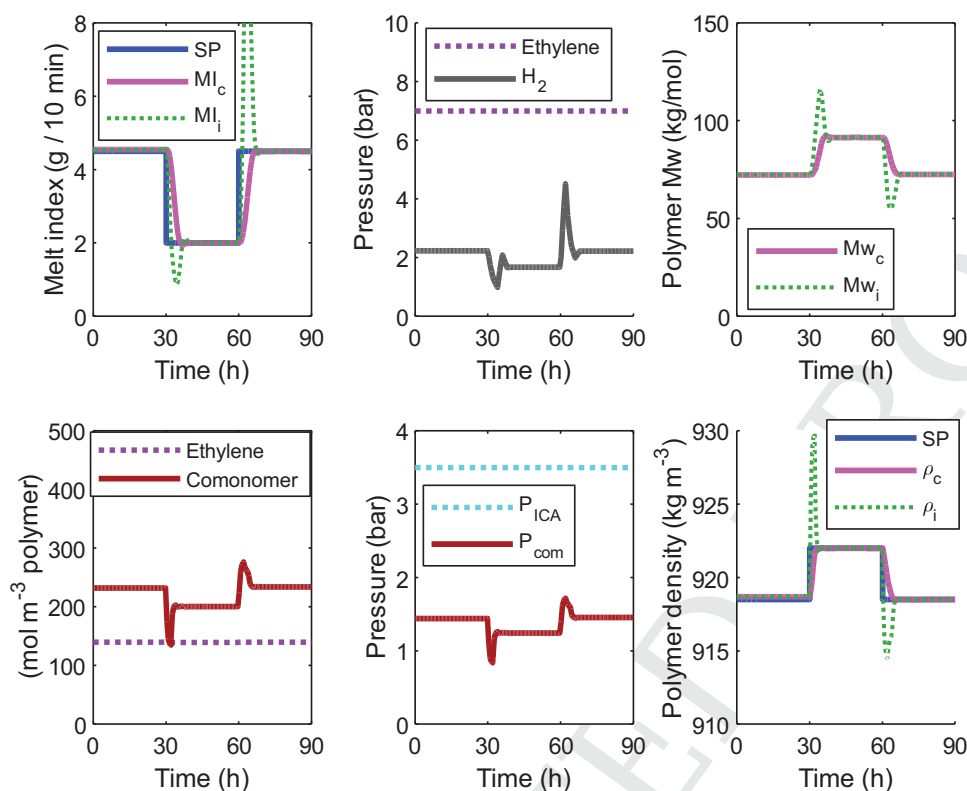


Figure 7. Grade transition in ethylene-1-butene copolymerization in presence of iso-butane ($\omega_1 = 0.08$, $\omega_2 = 1$, $\omega_3 = 8$, $\omega_4 = 19$, and $\omega_5 = 0$).

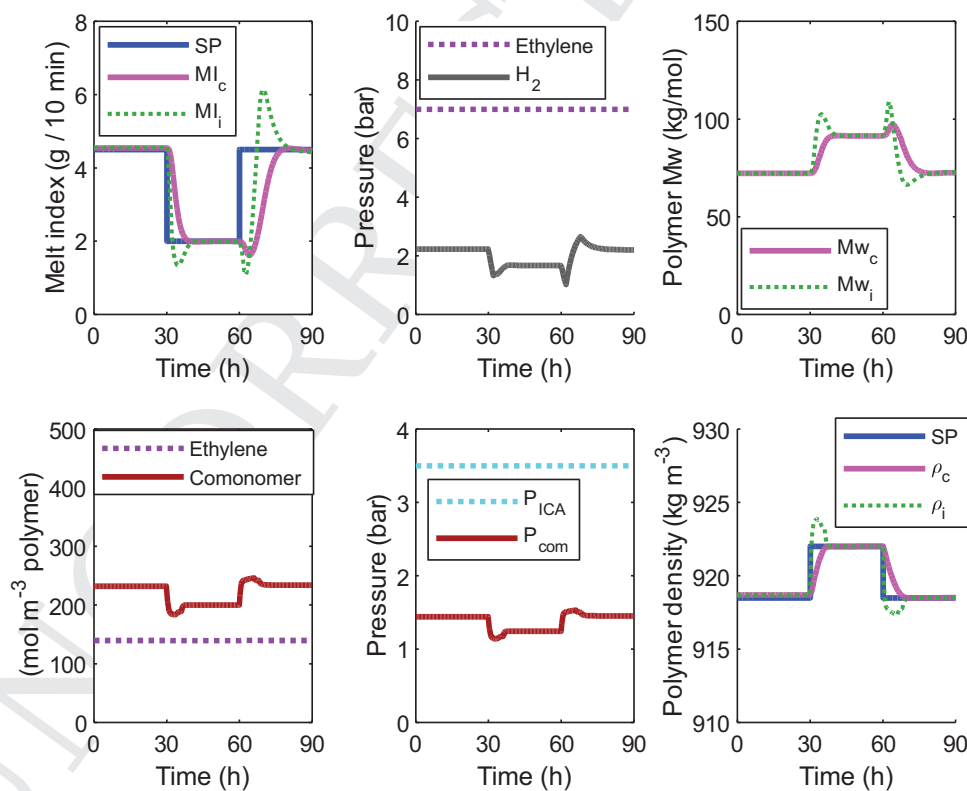


Figure 8. Grade transition in ethylene-1-butene: effect of the term $\omega_5 \sum_{i=1}^2 \frac{\Delta u_i}{u_i(t_0)}$ in the objective function ($\omega_1 = 0.08$, $\omega_2 = 1$, $\omega_3 = 8$, $\omega_4 = 19$, and $\omega_5 = 10^4$).

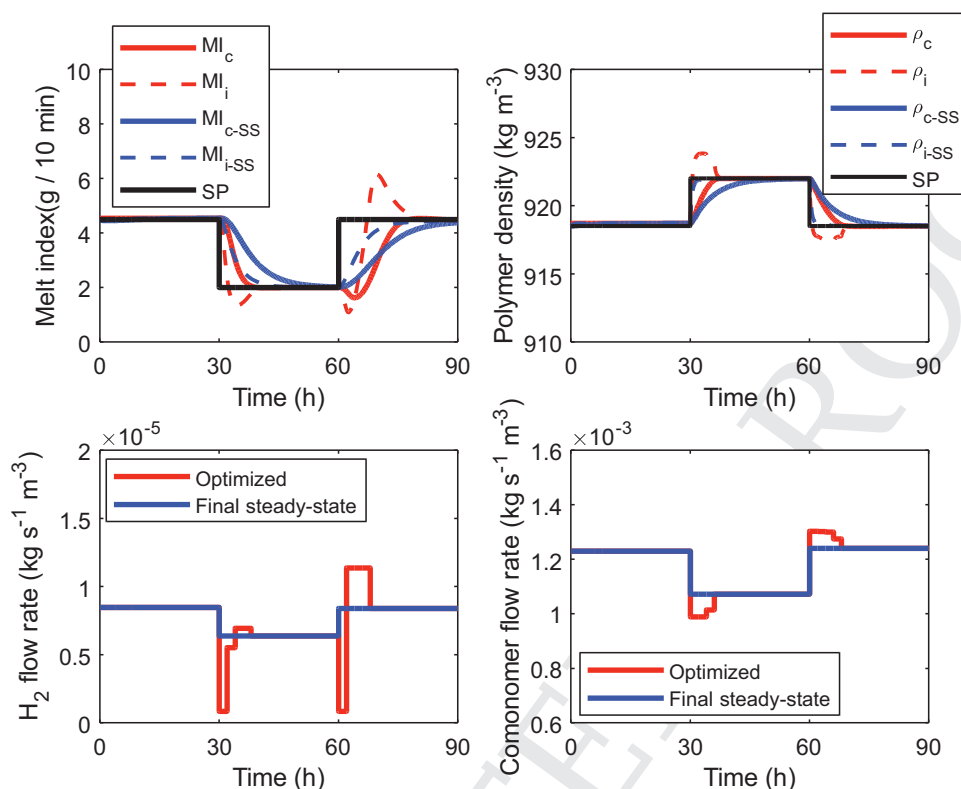


Figure 9. Grade transition in ethylene-1-butene copolymerization: comparison between the proposed grade transition strategy (leading to varying optimized flow rates during the transition) and injecting a constant flow rate during the transition (corresponding to the optimal flow rate of the final grade, under steady-state conditions).

time of the reactor. It can be seen that employing the optimized varying flow rates during the transition allows to reduce the convergence times of the cumulative melt index and the density.

4.3. Impact of the Thermodynamic Model

In order to demonstrate the importance of employing a good thermodynamic model in the optimization strategy, two scenarios were simulated. The first scenario was performed by assuming an error in the parameters of the thermodynamic model. The second system was used for this purpose, i.e., ethylene-1-butene copolymerization in presence of iso-butane as ICA.

In **Figure 10**, an error is assumed in the parameters A and E in Equations (1) and (2), related to the calculation of ethylene and comonomer concentrations in polymer, $[M_1^p]$ and $[M_2^p]$, respectively. It can be seen that the employed flow rates bring the process to different set-points than the desired ones (lower MI and ρ , as the used parameters A and E were assumed to be underestimated). Indeed, using lower A and E parameters in the model gives lower $[M_1^p]$ and $[M_2^p]$ than the real ones. In order to correct ratios of monomer to hydrogen as well as to comonomer (to obtain the desired properties), the optimization strategy forces the decrease in the hydrogen flow rate, which leads to an increase in the polymer molecular weight, and a decrease in the MI. Similarly, the optimization forces the

decrease in the comonomer flow rate, and as a result of errors in $[M_1^p]$ and $[M_2^p]$, a decrease in the polymer density is observed in this case. Note that the optimization strategy continues to work adequately, but as it is based on a wrong model it does not converge to the correct optimal points, therefore the use of an adequate thermodynamic model is essential.

The second scenario was performed by switching to a binary model to describe the solubility of the different species in the polymer (i.e., with no cosolubility effect). The system ethylene-1-hexene copolymerization in presence of *n*-hexane as ICA was used for this simulation. In this case, the thermodynamic model leads to the calculation of an incorrect concentration of ethylene in the amorphous phase of the polymer, $[M_1^p] = 257 \text{ mol m}^{-3}$ at 10 bar ethylene and 90 °C (as it assumes a binary system)^[27] instead of around 280 mol m⁻³ estimated in the pseudo-quaternary system. It also calculates an incorrect comonomer concentration in the polymer particle $[M_2^p]$. The concentration of 1-hexene in a binary system (1-hexene+LLDPE)^[29] is expected to be higher compared to its concentration in a ternary system due to the antisolvent effect of ethylene (as shown in **Figure 2**). However, combining ICA+comonomer in a pseudo-quaternary system leads to a global pressure which is much higher. As indicated by **Figure 4**, a small change in the pressure leads to a high change in the solubility of the pseudo-component, so the quaternary system leads to a much higher concentration of comonomer in the particles than in a binary system at the same pressure. Note however that the same flow rate is injected in the model and the process, but different reaction rates occur (due

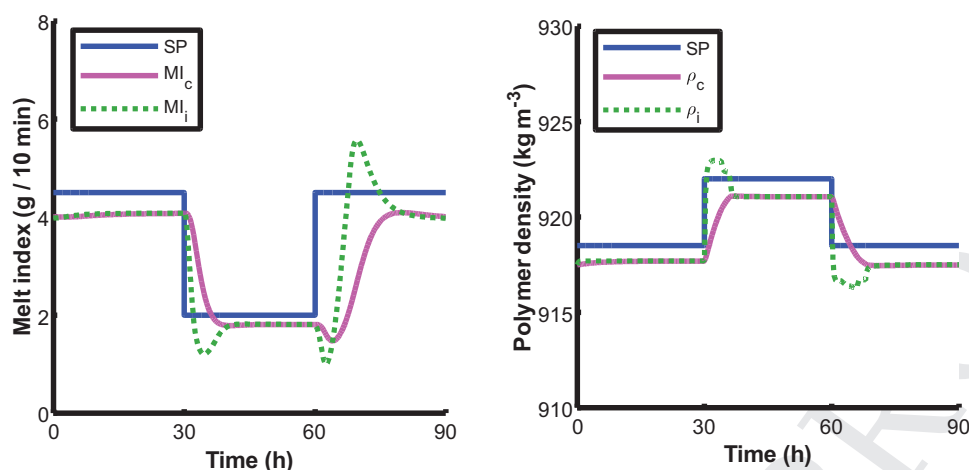


Figure 10. Influence of the thermodynamic model parameters on the process response, in ethylene and 1-butene copolymerization (Process parameters: $A = 1.98 \text{ mol m}^{-3} \text{ Pa}^{-1}$, $E = 180 \text{ mol m}^{-3}$, Model parameters used for optimization: $A = 0.992 \text{ mol m}^{-3} \text{ Pa}^{-1}$, $E = 90.2 \text{ mol m}^{-3}$).

to the use of different thermodynamic models), therefore the comonomer pressure varies a lot between the two simulations, and therefore it is not straightforward to compare the concentration of comonomer in the model and the process in this simulation. In this simulation, when $[M_2^p] = 165 \text{ mol m}^{-3}$ in the pseudo-quaternary system, it was $[M_2^p] = 159 \text{ mol m}^{-3}$ in the binary model.

The simulation test was performed using the binary model for both the concentrations of ethylene and 1-hexene in the amorphous phase of the polymer (so the model and grade transition is simulated using the binary model while the process is simulated using the pseudo-quaternary model). Figure 11 shows that using a binary thermodynamic model and ignoring the cosolubility effect leads to a big drift in the properties from the set-points. Indeed, the model assumes a lower $[M_1^p]$ (so a lower polymer molecular weight and a higher MI). Therefore, the optimization strategy based on this model makes the decision to decrease the hydrogen flow rate. However, when implemented to the process (simulated using the pseudo-quaternary

model, where the concentration of monomer is higher), this flow rate leads to a higher MW, so to a lower MI. Following the same reasoning, a drift in the polymer density occurs due to errors in both $[M_1^p]$ and $[M_2^p]$. This simulation demonstrates the importance of using an adequate thermodynamic model in the optimization strategy.

5. Conclusions

In this work, off-line dynamic optimization was implemented to optimize the grade transitions in a fluidized bed reactor of polyethylene. A combined kinetic and thermodynamic model was used in order to account for the cosolubility effects of the different gas species. The thermodynamic model is based on Sanchez-Lacombe EoS, but then simplified correlations were used to reduce the calculation time. Two copolymerizations were considered, the copolymerization of ethylene with 1-hexene in presence of *n*-hexane as ICA and the

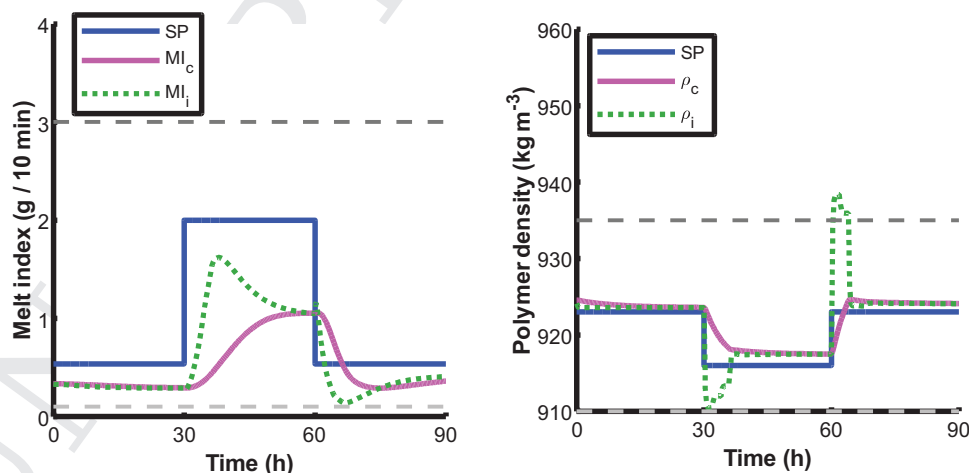


Figure 11. Influence of using binary thermodynamic model (not taking in account the cosolubility effect) on the process response. System ethylene-1-hexene copolymerization in presence of *n*-hexane at 90 °C. ($\omega_1 = 0.08$, $\omega_2 = 1$, $\omega_3 = 8$, $\omega_4 = 19$, and $\omega_5 = 10^4$).



1 copolymerization of ethylene with 1-butene in presence of iso-
2 butane. Some assumptions were made, mainly due to the lack
3 of thermodynamic data in the literature, to allow the prediction
4 of the solubility of the different species in PE in these quater-
5 nary systems.

6 The simulation results demonstrate the importance of the
7 thermodynamic model in the optimization strategy. A good
8 control of the polymer melt index and density could be realized
9 by manipulating the flow rates of hydrogen and comonomer.
10 Nevertheless, in both systems, the cosolubility effect of com-
11 oner on ethylene was not observed, which is due to the low
12 impact of the pseudo-component on the solubility of ethylene
13 under the employed operating conditions (pressure and tem-
14 perature). The importance of the thermodynamic model was
15 mainly related to evaluating the concentration of comonomer
16 in the polymer during the transition, which highly impacts the
17 polymer properties.

18 Both the instantaneous and the cumulative properties could
19 be controlled, in a duration much lower than the residence time
20 of the reactor. The role of the weighting factors, in the minimi-
21 zation function, is determinant at this level, where it can either
22 give more importance to controlling the instantaneous proper-
23 ties (thus eliminating any overshoot) or on the contrary allow a
24 faster control of the cumulative properties in detriment of the
25 instantaneous ones. A compromise between these two options
26 is necessary in order to ensure a fast convergence of the cumu-
27 lative properties to the set-points (thus reduce the transition
28 product) while avoiding big variations in the flow rates or pres-
29 sures of hydrogen and comonomer as they may increase the
30 risk of polymer sticking or softening. To reach the same objec-
31 tive, constraints on the instantaneous properties can be consid-
32 ered, but this slows down the calculation.

33 The proposed optimization tool should allow a more effi-
34 cient operation and a better control of the polymer quality. The
35 kinetic parameters and the correlations of the polymer prop-
36 erties used in this work were taken from literature, as well as
37 the assumption of the bed to behave as a CSTR. These models
38 can be replaced by more detailed models when available in the
39 same optimization strategy. For instance, improvement at the
40 level of the bed model can be done by considering a compart-
41 mental model and at the kinetic level by considering multiple
42 site catalysts leading to bimodal molecular weight distributions
43 and using correlations of the MI and polymer density adapted
44 to such systems. Finally, the availability of more thermody-
45 namic data or the use of a particle model accounting for diffu-
46 sion would allow to improve the precision of the optimization
47 strategy outcome.

50 Acknowledgements

51 This work was funded by Agence Nationale de la Recherche (Thermopoly
52 project, Grant No. ANR-16-CE93-0001-01). The authors would like
53 to thank M. Robert Pelletier for his input on grade transitions in
54 polymerization processes.

57 Conflict of Interest

58 The authors declare no conflict of interest.
59

Keywords

condensed mode cooling, fluidized bed reactor, grade transition,
polyethylene, thermodynamics

Received: March 23, 2020

Revised: May 8, 2020

Published online:

- [1] T. J. Hutley, M. Ouederni, *Polyolefin Compounds and Materials*, Springer International Publishing, Cham, Switzerland **2016**.
- [2] J. B. P. Soares, T. F. L. McKenna, *Polyolefin Reaction Engineering*, Wiley-VCH, Mannheim, Germany **2012**.
- [3] T. F. L. McKenna, *Macromol. React. Eng.* **2019**, *13*, 1800026.
- [4] J. M. JenkinsIII, R. L. Jones, T. M. Jones, S. Beret (Union Carbide Corp), *US Patent 4588790A*, **1986**.
- [5] A. Alizadeh, M. Namkajorn, E. Somsook, T. F. L. McKenna, *Macromol. Chem. Phys.* **2015**, *216*, 903.
- [6] A. Alizadeh, M. Namkajorn, E. Somsook, T. F. L. McKenna, *Macromol. Chem. Phys.* **2015**, *216*, 985.
- [7] J. A. Debling, G. C. Han, F. Kuijpers, J. Verburg, J. Zakka, W. H. Ray, *AIChE J.* **1994**, *40*, 506.
- [8] M. R. Rahimpour, J. Fathikalajahi, B. Moghtaderi, A. N. Farahani, *Chem. Eng. Technol.* **2005**, *28*, 831.
- [9] M. Ohshima, I. Hashimoto, T. Yoneyama, M. Takeda, F. Gotoh, *IFAC Proc.* **1994**, *27*, 505.
- [10] H. Seki, M. Ogawa, S. Ooyama, K. Akamatsu, M. Ohshima, W. Yang, *Control Eng. Pract.* **2001**, *9*, 819.
- [11] K. B. McAuley, *Ph.D. Thesis*, McMaster University, **1991**.
- [12] K. B. McAuley, J. F. MacGregor, *AIChE J.* **1992**, *38*, 1564.
- [13] M. Takeda, W. H. Ray, *AIChE J.* **1999**, *45*, 1776.
- [14] H.-S. Yi, J. H. Kim, C. Han, J. Lee, S.-S. Na, *Ind. Eng. Chem. Res.* **2003**, *42*, 91.
- [15] C. Chatzidoukas, J. D. Perkins, E. N. Pistikopoulos, C. Kiparissides, *Chem. Eng. Sci.* **2003**, *58*, 3643.
- [16] R. H. Nyström, R. Franke, I. Harjunkoski, A. Kroll, *Comput. Chem. Eng.* **2005**, *29*, 2163.
- [17] D. Bonvin, L. Bodizs, B. Srinivasan, *Chem. Eng. Res. Des.* **2005**, *83*, 692.
- [18] Y. Wang, H. Seki, S. Ohyama, K. Akamatsu, M. Ogawa, M. Ohshima, *Comput. Chem. Eng.* **2000**, *24*, 1555.
- [19] Y. Wang, G. S. Ostace, R. A. Majewski, L. T. Biegler, *IFAC-PapersOn-Line* **2019**, *52*, 448.
- [20] I. C. Sanchez, R. H. Lacombe, *Macromolecules* **1978**, *11*, 1145.
- [21] R. Alves, M. A. Bashir, T. F. L. McKenna, *Ind. Eng. Chem. Res.* **2017**, *56*, 13582.
- [22] P. A. Mueller, J. R. Richards, J. P. Congalidis, *Macromol. React. Eng.* **2011**, *5*, 261.
- [23] A. Alizadeh, *Ph.D. Thesis*, Queen's University, **2014**.
- [24] A. S. Michaels, H. J. Bixler, *J. Polym. Sci.* **1961**, *50*, 393.
- [25] M. A. Bashir, M. A.-H. Ali, V. Kanellopoulos, J. Seppälä, *Fluid Phase Equilib.* **2013**, *358*, 83.
- [26] F. Nascimento de Andrade, *Ph.D. Thesis*, University Claude Bernard Lyon 1, **2019**.
- [27] W. Yao, X. Hu, Y. Yang, *J. Appl. Polym. Sci.* **2007**, *103*, 1737.
- [28] H.-J. Jin, S. Kim, J.-S. Yoon, *J. Appl. Polym. Sci.* **2002**, *84*, 1566.
- [29] A. Novak, M. Bobak, J. Kosek, B. J. Banaszak, D. Lo, T. Widya, W. H. Ray, J. J. de Pablo, *J. Appl. Polym. Sci.* **2006**, *100*, 1124.
- [30] M. A. Bashir, V. Monteil, V. Kanellopoulos, M. A.-H. Ali, T. McKenna, *Macromol. Chem. Phys.* **2015**, *216*, 2129.
- [31] W. Yao, X. Hu, Y. Yang, *J. Appl. Polym. Sci.* **2007**, *104*, 3654.
- [32] W. M. R. Parrish, *J. Appl. Polym. Sci.* **1981**, *26*, 2279.
- [33] S. J. Moore, S. E. Wanke, *Chem. Eng. Sci.* **2001**, *56*, 4121.



- 1 [34] A. B. de Carvalho, P. E. Gloor, A. E. Hamielec, *Polymer* **1989**, 30, 280. 1
2 [35] K. B. McAuley, J. F. MacGregor, A. E. Hamielec, *AIChE J.* **1990**, 36, 837. 2
3 3
4 [36] J. Sun, H. Wang, M. Chen, J. Ye, B. Jiang, J. Wang, Y. Yang, C. Ren, 4
5 *J. Appl. Polym. Sci.* **2017**, 134. 5
6 [37] N. M. Ghasem, W. L. Ang, M. A. Hussain, *Korean J. Chem. Eng.* 6
7 **2009**, 26, 603. 7
8 [38] S. Chakravarti, W. H. Ray, *J. Appl. Polym. Sci.* **2001**, 80, 1096. 8
9 [39] A. Alizadeh, T. F. L. McKenna, *Macromol. Symp.* **2013**, 333, 242. 9
10 [40] H. Hatzantonis, H. Yiannoulakis, A. Yiagopoulos, C. Kiparissides, 10
11 *Chem. Eng. Sci.* **2000**, 55, 3237. 11
12 [41] P.-O. Larsson, J. Akesson, N. Andersson, presented at Proc. 50th 12
13 IEEE CDC-ECC, Orlando, FL, December **2011**. 13
14 [42] M. Ogawa, M. Ohshima, K. Morinaga, F. Watanabe, *J. Process Con-* 14
15 *trol* **1999**, 9, 51. 15
16 [43] A. Gisas, B. Srinivasan, D. Bonvin, *Comput.-Aided Chem. Eng.* 16
17 **2003**, 15, 463. 17
18 [44] A. Kiashemshaki, N. Mostoufi, R. Sotudeh-Gharebagh, 18
19 S. Pourmahdian, *Chem. Eng. Technol.* **2004**, 27, 1227. 19
20 [45] M. S. Abbas-Abadi, M. N. Haghighi, H. Yeganeh, *J. Appl. Polym. Sci.* 20
21 **2012**, 126, 1739. 21
22 22
23 23
24 24
25 25
26 26
27 27
28 28
29 29
30 30
31 31
32 32
33 33
34 34
35 35
36 36
37 37
38 38
39 39
40 40
41 41
42 42
43 43
44 44
45 45
46 46
47 47
48 48
49 49
50 50
51 51
52 52
53 53
54 54
55 55
56 56
57 57
58 58
59 59
- [46] V. Touloupides, V. Kanellopoulos, P. Pladis, C. Kiparissides, 1
2 D. Mignon, P. Van-Grambezen, *Chem. Eng. Sci.* **2010**, 65, 3208. 2
[47] M. F. Bergstra, G. Weickert, G. B. Meier, *Macromol. React. Eng.* 3
4 **2009**, 3, 433. 4
[48] J. Shi, L. T. Biegler, I. Hamdan, *AIChE J.* **2016**, 62, 1126. 5
[49] K. B. Sinclair, *Process Economics Report*, SRI International, Menlo 6
7 Park, CA **1983**. 7
[50] K. C. Seavey, Y. A. Liu, N. P. Khare, T. Bremner, C.-C. Chen, *Ind. Eng.* 8
9 *Chem. Res.* **2003**, 42, 5354. 9
[51] T. Bremner, A. Rudin, D. G. Cook, *J. Appl. Polym. Sci.* **1990**, 41, 10
11 1617. 11
[52] M. Embiruçu, D. M. Prata, E. L. Lima, J. C. Pinto, *Macromol. React.* 12
13 *Eng.* **2008**, 2, 142. 13
[53] A. J. Peacock, *Handbook of Polyethylene: Structures: Properties, and* 14
15 *Applications*, CRC Press, Boca Raton, FL **2000**. 15
[54] E. H. Lee, T. Y. Kim, Y. K. Yeo, *Korean J. Chem. Eng.* **2008**, 25, 16
17 613. 17
[55] C. Chatzidoukas, *Ph.D. Thesis*, University of London, **2004**. 18
[56] D. P. Lo, W. H. Ray, *Ind. Eng. Chem. Res.* **2006**, 45, 993. 19
[57] H.-S. Yi, J. H. Kim, C. Han, J. Lee, S.-S. Na, *Ind. Eng. Chem. Res.* 20
21 **2003**, 42, 91. 21
22 22
23 23
24 24
25 25
26 26
27 27
28 28
29 29
30 30
31 31
32 32
33 33
34 34
35 35
36 36
37 37
38 38
39 39
40 40
41 41
42 42
43 43
44 44
45 45
46 46
47 47
48 48
49 49
50 50
51 51
52 52
53 53
54 54
55 55
56 56
57 57
58 58
59 59

Macromolecular Reaction Engineering



Reprint Order Form

Editorial Office:
Wiley-VCH Verlag
Boschstraße 12, 69469 Weinheim
Germany
Tel.: +49 (0) 6201 – 606 – 581
Fax: +49 (0) 6201 – 606 – 510
Email: macromol@wiley-vch.de

Manuscript No.: _____
Customer No.: (if available) _____
Purchase Order No.: _____
Author: _____

Charges for Reprints in Euro (excl. VAT), prices are subject to change. Minimum order 50 copies.

No. of pages	50 copies	100 copies	150 copies	200 copies	300 copies	500 copies
1–4	345,—	395,—	425,—	445,—	548,—	752,—
5–8	490,—	573,—	608,—	636,—	784,—	1077,—
9–12	640,—	739,—	786,—	824,—	1016,—	1396,—
13–16	780,—	900,—	958,—	1004,—	1237,—	1701,—
17–20	930,—	1070,—	1138,—	1196,—	1489,—	2022,—
every additional 4 pages	147,—	169,—	175,—	188,—	231,—	315,—

Information regarding VAT: The charges for publication of *cover pictures/reprints/issues/poster/Video abstracts/* are considered to be “supply of services” and therefore subject to German VAT. However, if you are an institutional customer outside Germany, the tax can be waived if you provide us with the valid VAT number of your company. Non-EU customers may have a VAT number starting with “EU” instead of their country code, if they are registered with the EU tax authorities. If you do not have a valid EU VAT number and you are a taxable person doing business in a non-EU country, please provide a certification from your local tax authorities confirming that you are a taxable person under local tax law. Please note that the certification must confirm that you are a taxable person and are conducting an economic activity in your country. **Note:** certifications confirming that you are a tax-exempt legal body (non-profit organization, public body, school, political party, etc.) in your country do not exempt you from paying German VAT.

Please send me send bill me for

- no. of reprints
 high-resolution PDF file (330 Euro excl. VAT)
E-mail address: _____

❖ Special Offer:

If you order 200 or more reprints you will get
a PDF file for half price.

*Please note: It is not permitted to present the PDF file on
the internet or on company homepages.*

Cover Posters (prices excl. VAT)

Posters of published covers are available in two sizes:

- DinA2 42 x 60 cm / 17 x 24in (one copy: 39 Euro)
 DinA1 60 x 84 cm / 24 x 33in (one copy: 49 Euro)

Postage for shipping (prices excl. VAT)

overseas +25 Euro
within Europe +15 Euro

VAT number: _____

Mail reprints / copies of the issue to:

Send bill to:

I will pay by bank transfer

I will pay by credit card

VISA, Mastercard and AMERICAN EXPRESS

For your security please use this link (Credit Card
Token Generator) to create a secure code Credit
Card Token and include this number in the form
instead of the credit card data. Click here:

https://www.wiley-vch.de/editorial_production/index.php

CREDIT CARD TOKEN NUMBER

						V													
--	--	--	--	--	--	---	--	--	--	--	--	--	--	--	--	--	--	--	--

Date, Signature _____